Electronic Supplementary Material (ESI) for Green Chemistry.

Supporting Information

Heavy metal recovery from electroplating wastewater by synthesis of the mixed-Fe_3O_4@SiO_2/metal oxide magnetite photocatalysts

Shouqiang Huang, Lin Gu, Nanwen Zhu,* Kaili Feng, Haiping Yuan, Ziyang Lou,* Yiqun Li, and Aidang Shan

School of Environmental Science and Engineering, Shanghai Jiao Tong University, Dongchuan Road 800, 200240, Shanghai, P. R. China.

Corresponding Author: Phone/Fax: +86 21 54743710; Email: nwzhu@sjtu.edu.cn; louworld12@sjtu.edu.cn.

Preparation of M-Fe_3O_4 nanoparticles from EPW

200 mL of S-EPW was placed into a 250 mL beaker, and its pH was adjusted to 2 using H_2SO_4 solution (3 mol L^{-1}) under continuous stirring. Then, $FeSO_4 \cdot 7H_2O$ was introduced to reduce Cr^{6+} in EPW and provided Fe^{2+} for ferrites, and the optimum ratio of $FeSO_4 \cdot 7H_2O$: Cr^{6+} was tested with the mass ratios of 30: 1, 50: 1, 100: 1, 200: 1, and 300: 1 in series. After the reduction of Cr^{6+} for 15 min, NaOH solution (6 mol L^{-1}) was dropped to increase the pH to 10. Then the beaker was sealed and stored in a thermostat water bath at 80 ºC for 10 h. The precipitates were separated by centrifugation, washed with distilled water and ethanol, and then dried in vacuum at 60 ºC for 10 h to form the M-Fe_3O_4 products.

Preparation of M-Fe_3O_4@SiO_2 core-shell nanoparticles

In a typical procedure, 0.02 g M-Fe_3O_4 nanoparticles were dispersed in 80 mL ethanol under sonication for 10 min, and then the mixture was transferred to a three-necked flask with continuous mechanical stirring (200 rpm). 20 mL deionized water, 2.32 mL aqueous ammonia (mass fraction of 25%), and 0.45 mL tetraethyl orthosilicate (the density of 0.932 g mL^{-1}) were introduced and mixed together at room temperature. After 6 h, the M-Fe_3O_4@SiO_2 nanoparticles were collected via centrifugation and dried in vacuum at 60 ºC for 10 h.

Leaching test

The Toxicity Characteristic Leaching Procedure (TCLP) was used to assess the chemical stability of the M-Fe_3O_4 products. Accordingly, distilled water with a pH of 4.93 ± 0.05 was used as the extraction fluid with a liquid-to-solid ratio of 20: 1. The obtained mixtures were shaken at a rate of 30 ± 2 rpm for 18 h, and then the leachate was filtered and determined with ICP.[1, 2]

XRD and magnetic analysis of M-Fe_3O_4

The crystal phases of the as-prepared M-Fe_3O_4 samples are shown in Fig. S1a, and the phases of Fe_3O_4, $FeCr_2O_4$, $ZnFe_2O_4$, and $CuFe_2O_4$ are mainly found in the M-Fe_3O_4 products. Among them, Fe_3O_4 and $CuFe_2O_4$ possess the inverse spinel structure,[3, 4] while $FeCr_2O_4$ and $ZnFe_2O_4$ exhibit the normal spinel structure.[5, 6] In the preparation process of M-Fe_3O_4, the reduction of Cr^{6+} is first occurred with the addition of $FeSO_4 \cdot 7H_2O$, and the reaction can be expressed as Eq. (1):

$$Cr_2O_7^{2-} + 6Fe^{2+} + 14H^+ \rightarrow 2Cr^{3+} + 6Fe^{3+} + 7H_2O \quad (1)$$

Then, the amount of Cr^{3+} and Fe^{3+} ions are increased, accompanied by the decreased Fe^{2+} content, while the Cu^{2+}, Zn^{2+}, and Ni^{2+} ions can substitute Fe^{2+} ions to form M-Fe_3O_4, and thus the principle of the ferrite process can be presented in Eq. (2-5):[7]

$$Fe^{2+} + 2Fe^{3+} + 8OH^- \rightarrow Fe_3O_4 + 4H_2O \quad (2)$$

$$Zn^{2+} + 2Fe^{3+} + 8OH^- \rightarrow ZnFe_2O_4 + 4H_2O \quad (3)$$

$$Cu^{2+} + 2Fe^{3+} + 8OH^- \rightarrow CuFe_2O_4 + 4H_2O \quad (4)$$

$$Fe^{2+} + 2Cr^{3+} + 8OH^- \rightarrow FeCr_2O_4 + 4H_2O \quad (5)$$

According to the increased added amount of $FeSO_4 \cdot 7H_2O$, the following reaction may also occur as Eq. (6):[8]

$$\chi\, Me^{2+} + (3-\chi)\, Fe^{2+} + 6OH^- + 1/2O_2 \rightarrow Me_\chi Fe_{(3-\chi)}O_4 + 3H_2O \quad (6)$$

In the XRD patterns, there is no diffraction peak for $NiFe_2O_4$, since the mass concentration of Ni^{2+} in S-EPW is too low (4 mg L^{-1}). In addition, the diffraction peak intensities of M-Fe_3O_4 are first increased and then decreased as the mass ratios of $FeSO_4 \cdot 7H_2O$: Cr^{6+} increased from 30: 1 to 300: 1, which are in conformity with the magnetic properties of M-Fe_3O_4 (Fig. S1b). Theoretically, the needed mass ratio of $FeSO_4 \cdot 7H_2O$: Cr^{6+} is 23: 1, and Fe^{2+} will be easily oxidized to Fe^{3+} in the practical condition where exposed to air. In the case of low mass ratio (30: 1), poor crystal quality of M-Fe_3O_4 is observed, combined with a small saturated magnetization (M_s) of 5.94 emu g^{-1} and a high coercivity (H_c) of 145.5 O_e (Table S2). In contrast, a higher crystallization degree is obtained in the mass ratio of 50: 1, where the M_s and H_c values are 55.05 emu g^{-1} and 55.67 O_e, respectively. If the mass ratios increased further, the M_s values of M-Fe_3O_4 are not changed much, i.e., 54.90 (100: 1), and 69.42 emu g^{-1} (200: 1), and higher H_c values are presented, which will increase the trend of aggregation for the M-Fe_3O_4 nanoparticles. On the other hand, both of them are not cost-efficient, since more Fe^{2+} ions are consumed, compared to the cases with lower mass ratios. Furthermore, Cr, Cu, Zn, and Ni ions in M-Fe_3O_4 prepared with the mass ratio of 50: 1 are more stable than those in other M-Fe_3O_4 samples (Table S3). Based on the above results, the mass ratio of 50: 1 is the best one for M-Fe_3O_4 preparation, and the obtained M-Fe_3O_4 products are chosen as the supports for the metal oxide photocatalysts in this work.

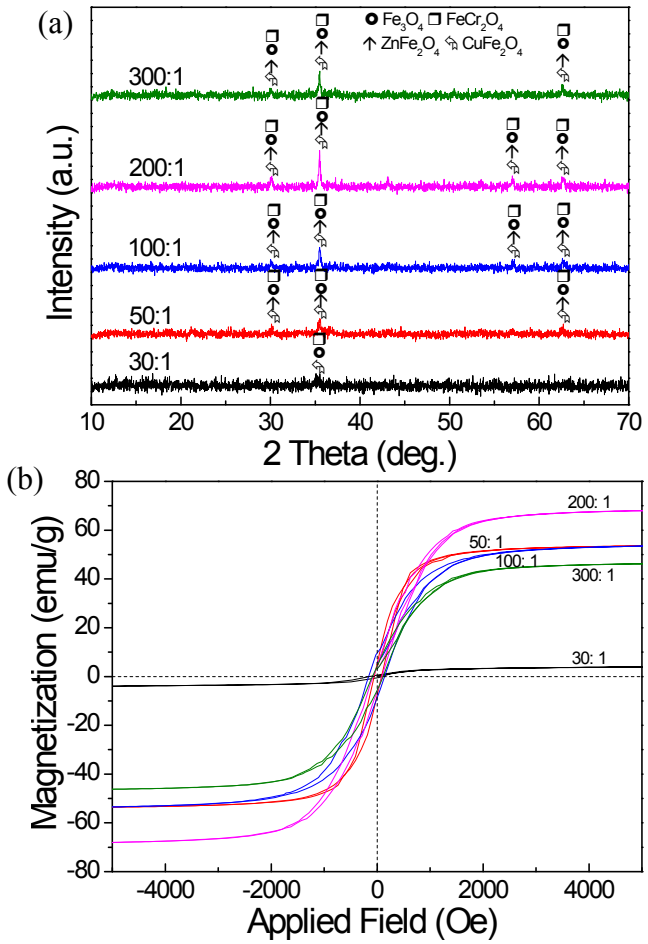

Fig. S1 (a) XRD patterns and (b) room temperature (300 K) magnetic hysteresis loops of M-Fe_3O_4 prepared with various mass ratios of $FeSO_4 \cdot 7H_2O$: Cr^{6+}.

Table S1. Heavy metal concentrations in supernatant liquors before and after the precipitation reactions.

Elements	Cr	Cu	Zn	Ni	Fe	pH	COD_{Cr}
R-EPW	113.36	98.04	60.92	2.59	15.60	2.34	270
R-EPW after precipitation	2.15	0.02	UD	0.02	UD	-	185
Recovery rate (%)	98.1	99.9	100	99.2	100	-	-
S-EPW	118.22	89.67	49.46	3.93	19.86	-	-
S-EPW after precipitation	1.20	0.01	UD	UD	UD	-	-
Recovery rate (%)	98.9	99.9	100	100	100	-	-

Note:

UD: Below detection limit.

All the parameters are expressed in mg L^{-1} except pH and recovery rate (%). The Cr^{6+} content in R-EPW was detected to be 101.27 mg L^{-1} by the 1, 5-diphenylcarbohydrazide spectrophotometric method.[9] The chemical oxygen demand (COD_{Cr}) of R-EPW was measured using the potassium dichromate method.

Table S2 Magnetic parameters of M-Fe_3O_4 prepared with various mass ratios of $FeSO_4 \cdot 7H_2O$: Cr^{6+}.

Samples	M_s (emu g^{-1})	H_c (Oe)
30: 1	5.94	145.5
50: 1	55.05	55.67
100: 1	54.90	158.45
200: 1	69.42	73.18
300: 1	47.55	87.56

Table S3 Chemical stability of the M-Fe_3O_4 products prepared with various mass ratios of $FeSO_4 \cdot 7H_2O$: Cr^{6+}.

Mass ratios of $FeSO_4 \cdot 7H_2O$: Cr^{6+}	Heavy metal concentration (mg L^{-1})			
	Cr	**Cu**	**Zn**	**Ni**
30: 1	UD	0.20	1.25	0.17
50: 1	UD	2.70	5.89	2.82
100: 1	0.79	40.00	9.21	3.72
200: 1	UD	20.90	3.37	3.94
300: 1	0.42	31.00	2.41	3.02
TCLP Standard[a]	5.00	15.00	-	-

Note:

UD: Below detection limit.

[a] Ref: D. Chen, J. Hou, L. H. Yao, H. M. Jin, G. R. Qian and Z. P. Xu, *Sep. Purif. Technol.*, 2010, **75**, 210.

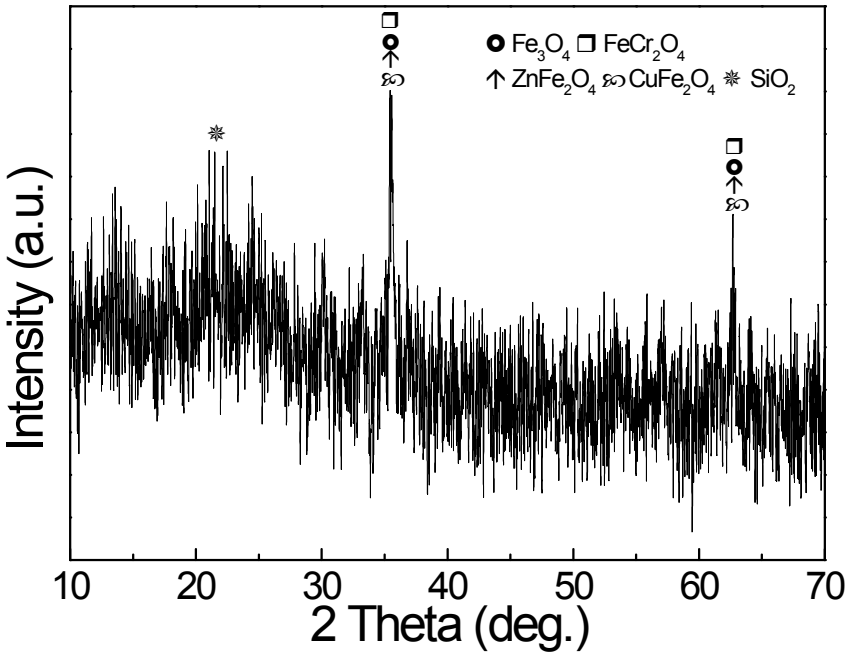

Fig. S2 XRD pattern of M-Fe_3O_4@SiO_2.

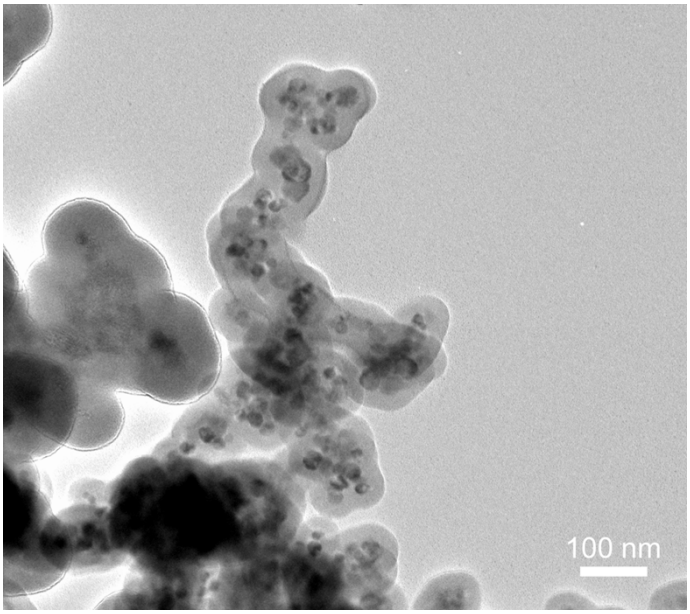

Fig. S3 TEM image of M-Fe_3O_4@SiO_2.

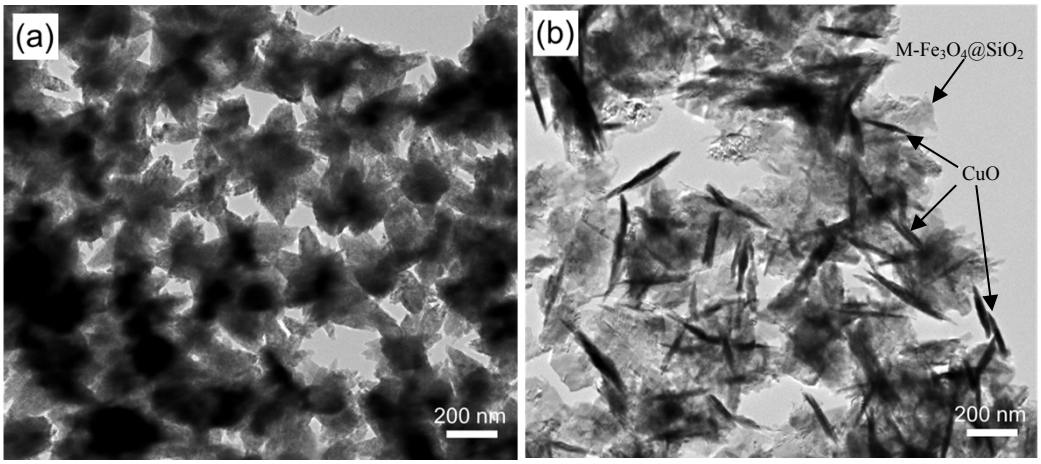

Fig. S4 TEM images of (a) M-Fe_3O_4@SiO_2/ZnO, and (b) M-Fe_3O_4@SiO_2/CuO.

Table S4 Physical parameters of the M-Fe_3O_4@SiO_2/metal oxides.

Samples	Band gap energy (eV)	Absorption edge (nm)	BET (m^2 g^{-1})	Pore size (nm)
M-Fe_3O_4@SiO_2/ZnO	3.15	393.65	15	3.37
M-Fe_3O_4@SiO_2/CuO	2.03	610.84	18	3.37
M-Fe_3O_4@SiO_2/Fe_2O_3	2.10	590.48	16	24.5
M-Fe_3O_4@SiO_2/NiO	3.53	351.27	177	4.23

Table S5 Magnetic parameters of M-Fe_3O_4, M-Fe_3O_4@SiO_2 and the M-Fe_3O_4@SiO_2/metal oxides.

Samples	M_s (emu g^{-1})	H_c (Oe)
M-Fe_3O_4 (50: 1)	55.05	55.67
M-Fe_3O_4@SiO_2	17.91	71.04
M-Fe_3O_4@SiO_2/ZnO	0.30	30.39
M-Fe_3O_4@SiO_2/CuO	0.49	74.74
M-Fe_3O_4@SiO_2/Fe_2O_3	23.03	182.29
M-Fe_3O_4@SiO_2/NiO	2.28	53.83

Table S6 Chemical element contents of M-Fe_3O_4@SiO_2/ZnO and M-Fe_3O_4@SiO_2/CuO obtained from XPS and EDS.

Elements	M-Fe_3O_4@SiO_2/ZnO	M-Fe_3O_4@SiO_2/CuO	
	EDS	XPS	EDS
Zn content (wt %)	76.98	-	-
Cu content(wt %)	-	46.24	47.48
Si content(wt %)	0.33	4.01	0.16
O content(wt %)	18.18	-	16.74
Fe content(wt %)	0.19	-	0.38

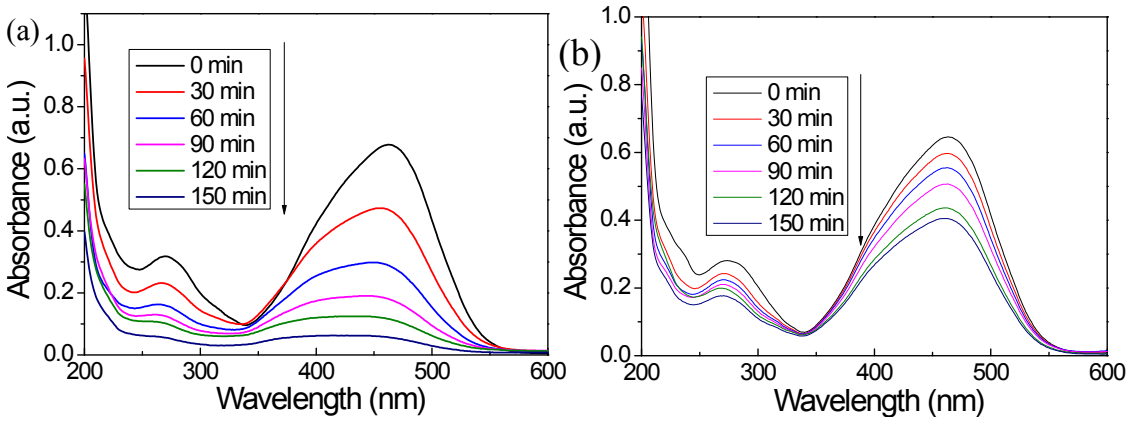

Fig. S5 Time-dependent absorption spectra of MO over (a) M-Fe_3O_4@SiO_2/ZnO and (b) M-Fe_3O_4@SiO_2/NiO under UV-vis irradiation.

Table S7 Degradation rates of the as-prepared Fe_3O_4@SiO_2/metal oxides.

Samples	Degradation rates (%) after 150 min
M-Fe_3O_4@SiO_2/ZnO, 1.00 g L^{-1}	91.5
M-Fe_3O_4@SiO_2/CuO, 0.50 g L^{-1}	17.6
M-Fe_3O_4@SiO_2/CuO, 1.00 g L^{-1}	3.4
M-Fe_3O_4@SiO_2/Fe_2O_3, 1.00 g L^{-1}	19.0
M-Fe_3O_4@SiO_2/NiO, 1.00 g L^{-1}	37.4
P-Fe_3O_4@SiO_2/Fe_2O_3, 1.00 g L^{-1}	16.6
M-Fe_3O_4@SiO_2/S-metal oxides, 1.00 g L^{-1}	17.4
M-Fe_3O_4@SiO_2/R-metal oxides, 1.00 g L^{-1}	13.2
P25, 1.00 g L^{-1}	95.4

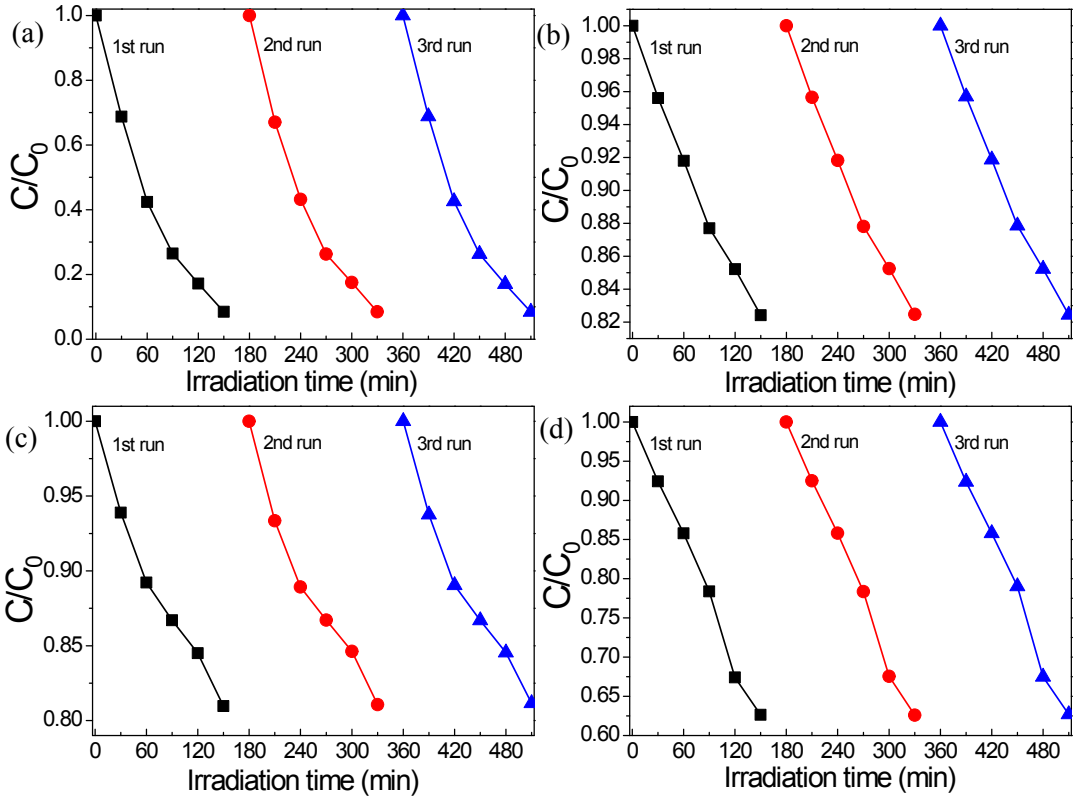

Fig. S6 Recycling photocatalytic degradations of MO over (a) M-Fe_3O_4@SiO_2/ZnO (1.00 g L^{-1}), (b) M-Fe_3O_4@SiO_2/CuO (0.50 g L^{-1}), (c) M-Fe_3O_4@SiO_2/Fe_2O_3 (1.00 g L^{-1}), (d) P-Fe_3O_4@SiO_2/NiO (1.00 g L^{-1}) under UV-vis light irradiation.

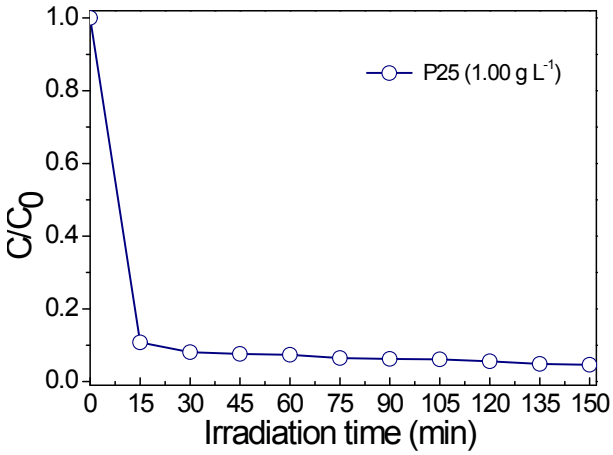

Fig. S7 Photocatalytic degradation of MO over P25 (Degussa, specific surface area of 50 m^2 g^{-1}) (1.00 g L^{-1}). The MO degradation rate of the commercial Degussa P25 titania is 95.4%, a little higher than that (91.5%) of M-Fe_3O_4@SiO_2/ZnO, while it is unable to reuse by magnetic recovery in the treated wastewater, and thus a certain advantage is displayed with the magnetite photocatalysts of the M-Fe_3O_4@SiO_2/metal oxides.

References

1 U.S. EPA, *Test Methods for Evaluating Solid Waste Physical/Chemical Methods*, EPA SW-846, 3rd edn., Method 1311-1, National Service Centre for Environmental Publications, Cincinnati, OH, 1996.

2 D. Chen, J. Hou, L. H. Yao, H. M. Jin, G. R. Qian and Z. P. Xu, *Sep. Purif. Technol.*, 2010, **75**, 210.

3 C. Hui, C. M. Shen, T. Z. Yang, L. H. Bao, J. F. Tian, H. Ding, C. Li and H. J. Gao, *J. Phys. Chem. C*, 2008, **112**, 11336.

4 Z. H. Xiao, S. H. Jin, X. K. Wang, W. Z. Li, J. H. Wang and C. H. Liang. *J. Mater. Chem.*, 2012, **22**, 16598.

5 A. Chartier, B. Golovchuk, S. Gossé and L. Van Brutzel, *J. Chem. Phys.*, 2013, **139**, 134702.

6 S. N. Rishikeshi, S. S. Joshi, M. K. Temgire and J. R. Bellare, *Dalton Trans.*, 2013, **42**, 5430.

7 E. Barrado, F. Prieto, M. Vega and F. Fernandez-Polanco, *Water Res.*, 1998, **32**, 3055.

8 M. Erdem and F. Tumen, *J. Hazard. Mater.*, 2004, **109**, 71.

9 Agency, C. N. E. P. Methods of Water and Wastewater Monitoring and Analysis; Chinese Environmental Science Publication: Beijing, 1994.